SOLUTION MINING RESEARCH INSTITUTE
105 Apple Valley Circle
Clarks Summit, PA 18411, USA

Telephone: +1 570-585-8092
Fax: +1 570-585-8091
www.solutionmining.org ◆ smri@solutionmining.org

Technical Conference Paper

Onset of tensile effective stresses in gas storage caverns

Benoit Brouard, Brouard Consulting, Paris, France
Pierre Bérest, Ecole Polytechnique, Palaiseau, France
Mehdi Karimi-Jafari, Ecole Polytechnique, Palaiseau, France

Fall 2007 Conference
7-10 October
Halifax, Canada

Solution Mining Research Institute, Fall 2007 Technical Meeting
Halifax, Canada, October 8-10, 2007

ONSET OF TENSILE EFFECTIVE STRESSES IN GAS STORAGE CAVERNS

Benoît Brouard[1], Pierre Bérest[2] Mehdi Karimi-Jafari[2]

[1] Brouard Consulting, Paris, France
[2] LMS, Ecole Polytechnique, Palaiseau, France

Abstract

In this paper, the effect of a rapid pressure build-up, as is observed in a gas cavern experiencing large yearly pressure cycles, is discussed. It is proved that such build-up leads to the onset of tensile effective stresses at the cavern wall.Three different constitutive models are considered, and computations are performed for the case of a 1500-m deep cavern. It is proved that the extent of the tensile effective zone is not extremely sensitive to pressure build-up rate. This zone becomes larger when the cavern experiences a large number of cycles.

Introduction

The structural stability of salt caverns must be assessed through numerical computation. Stresses, strains and volume changes are computed and compared to safety criteria. The following criteria often are considered:

(1) no, or small, dilatant zone;

(2) no, or small, tensile zone;

(3) limited volume loss and volume loss rate; and

(4) limited subsidence.

- A large dilatant zone must be avoided, as it is suspected that, in such a zone, salt softens, possibly leading to strain localization in shear zones. This criterion commonly is used to assess cavern stability (DeVries et al., 2003; Rokhar et al., 2004; Nieland and Ratigan, 2006; DeVries et al., 2006) or dry-mine stability (Minkley et al., 2007; Kamlot et al., 2007). It has been used successfully to back-analyze the mechanical behaviour of mines that had experienced the onset of sinkholes at ground level or panel collapse (Bauer et al., 2000; Bérest et al., 2007).

- Tensile zones must be avoided. The tensile strength of salt is low, and large tensile stresses lead to roof or wall spalling. In a salt cavern, stresses in the rock mass generally are compressive, and the criterion is satisfied. Outstanding exceptions are found when the cavern fluid pressure is low and the cavern profile exhibits non-convex portions. (An example of this is described in Nieland and Ratigan, 2006).

- Cavern volume loss and subsidence are closely related. Subsidence is of special concern for cavern fields when the distance between neighbouring caverns is small.

In the following, we suggest **a fifth criterion**:

(5) no, or limited, *effective* tensile zone.

By "effective stress", we mean the actual stress plus the fluid pressure in the pores of the rock. For a salt cavern, this quantity is defined easily at the cavern wall, because pore pressure simply is the cavern fluid pressure. The "effective stress" inside the rock mass is more difficult to define. On one hand, pore pressure is difficult to assess, especially in a gas-filled cavern; on the other hand, it is suspected that, in a rock whose porosity is small, the effective stress is the sum of the actual stress plus the fluid pressure multiplied by a factor smaller than 1 (Biot's coefficient). How these notions, which are classical in Reservoir Engineering, apply in the case of salt is a matter still open to discussion.

If we focus on the cavern wall, most authors accept that the effective stress must be smaller than a positive quantity, often called the rock tensile strength. The related criterion can be written:

$$\sigma_{\min} + P < T$$

where T is the rock tensile strength (Bérest et al., 2001a-2001b; Malinsky, 2001; Stormont, 2001; Rokhar et al., 1997). When this criterion is met, micro-fracturing occurs, permeability drastically increases, and salt softens. Selecting $T = 0$ (to be on the safe side), the criterion can be stated simply: the effective stress must be negative — i.e., "no tensile effective stress" must exist.

Tensile effective stresses are likely to develop at the cavern wall when cavern pressure experiences a large and rapid increase. For this reason, gas-storage caverns, in which gas pressure experiences large pressure cycles, are more prone to develop tensile stresses. A simplified closed-form solution allows explanation of this notion.

A Closed-Form Solution

The mechanical behaviour of salt is highly non-linear. Simulation of cavern behaviour as a function of time and cavern pressure history generally requires heavy numerical computations. Closed-form solutions are only possible when idealized spherical or cylindrical cavern shapes are considered, and when cavern history is simplified to the extreme. However, even when over-simplifying, closed-form solutions allow some aspects of the complex behaviour of actual caverns to be captured.

Consider the case of an idealized **spherical cavern.** The Norton-Hoff constitutive law is selected to describe the salt mechanical behaviour. Cavern pressure is decreased very slowly (so slowly that steady state can be reached at any instant) to a figure P_c^0. Steady-state then is reached. In particular, the stress distribution in the rock mass can be written as

$$\begin{cases} \sigma_{rr}^0(r) = -P_\infty + \left(P_\infty - P_c^0\right)(a/r)^{3/n} \\ \sigma_{\theta\theta}^0(r) = \sigma_{\varphi\varphi}^0 = -P_\infty + (1 - 3/2n)\left(P_\infty - P_c^0\right)(a/r)^{3/n} \end{cases} \quad (1)$$

where P_∞ is the geostatic pressure at cavern depth, n is the stress exponent of the Norton-Hoff power law ($n = 3$ to 6 is typical), a is the cavern radius, and r is the distance from the center of the sphere.

Now, two loadings are considered:

(1) cavern pressure drops by $-\Delta P = P_c - P_c^0 < 0$, or

(2) cavern pressure increases by $\Delta P = P_c - P_c^0 > 0$.

When these loadings or unloadings are extremely rapid, they generate additional elastic stresses; immediately after the cavern pressure change, stresses distribution can be written as

$$\begin{cases} \sigma_{rr}^{0}(r) = -P_{\infty} + \left(P_{\infty} - P_c^{0}\right)(a/r)^{3/n} - \left(P_c - P_c^{0}\right)(a/r)^{3} \\ \sigma_{\theta\theta}^{0}(r) = \sigma_{\varphi\varphi}^{0}(r) = -P_{\infty} + (1-3/2n)\left(P_{\infty} - P_c^{0}\right)(a/r)^{3/n} + 0.5\,\left(P_c - P_c^{0}\right)(a/r)^{3} \end{cases} \tag{2}$$

This stress distribution must be compared to a failure criterion. Two distinct criteria, related to the cavern pressure history, must be discussed: (1) decrase in cavern pressure and (2) increase in cavern pressure.

When cavern pressure drops ($P_c < P_c^0$), dilation can appear at cavern wall and in the rock mass. Dilation must be avoided, or minimized, as it generates strength-softening and permeability increase. Dilation criteria often are a function of two stress invariants, I_1 and J_2.

In particular, at the cavern wall, or $r = a$:

$$I_1(a) = \sigma_{rr}(a) + \sigma_{\theta\theta}(a) + \sigma_{\varphi\varphi}(a) = -3\left[\left(P_{\infty} - P_c^{0}\right)/n + P_c^{0}\right] \tag{3}$$

$$\sqrt{J_2(a)} = \frac{1}{\sqrt{3}}\left|\sigma_{rr}(a) - \sigma_{\theta\theta}(a)\right| = \frac{\sqrt{3}}{2}\left[\left(P_{\infty} - P_c^{0}\right)/n + \left(P_c^{0} - P_c\right)\right] \tag{4}$$

Simple criteria were proposed by Spiers et al. (1988) and Ratigan et al. (1991) for the onset of dilation:

$$\sqrt{J_2} < C_1\left|I_1\right| + C_2 \tag{5}$$

Criteria paramaters are given in Table 1.

Table 1 - Parameters for simple dilation criteria.

Authors	C_1	C_2 (MPa)
Spiers et al.	0.27	1.9
Ratigan et al.	0.27	0

Dilation appears at the cavern wall when

$$\sqrt{J_2} - C_1\left|I_1\right| - C_2 = \frac{\sqrt{3}}{2}\left[P_{\infty}\left(1 - 2\sqrt{3}C_1\right)/n + P_c^{0}\left(1 - 2\sqrt{3}C_1\right)(1 - 1/n) - P_c\right] - C_2 = 0 \tag{6}$$

When cavern pressure increases ($P_c > P_c^0$), tensile effective stresses may appear. Tensile effective stresses must be avoided or minimized, as they generate micro-fracturing and permeability increase (Fokker, 1995; Popp et al., 2007). The micro-fracturing criterion generally can be written:

$$\sigma_{\min} + P_c < T \tag{7}$$

where $\sigma_{\min}$ is the smallest compressive stress (Tension is positive, $\sigma_{\max} < \sigma_{\text{int}} < \sigma_{\min} < 0$.) ,and T is the rock-mass tensile strength. In general, T is small (a few MPa). At the cavern wall, tensile effective stresses appear when

$$\sigma_{\theta\theta}(r = a) + P_c = \frac{3}{2}\left[\left(P_c - P_c^{0}\right) - \left(P_{\infty} - P_c^{0}\right)/n\right] = T \tag{8}$$

The two criteria are drawn on Figure 1, which displays the dilatant domain and the tensile effective stress domain in the P_c^0/P_∞ (initial cavern pressure) versus P_c/P_∞ (final cavern pressure) plane. A value of the initial pressure, or P_c^0/P_∞, can be selected (represented by a dot on the first diagonal). Then, P_c/P_∞ increases or decreases. When P_c/P_∞ increases, tensile effective stresses develop — provided that the initial cavern pressure, or P_c^0/P_∞, is not too close to 1. It is remarkable that tensile effective stress develops even when cavern pressure is far below geostatic.

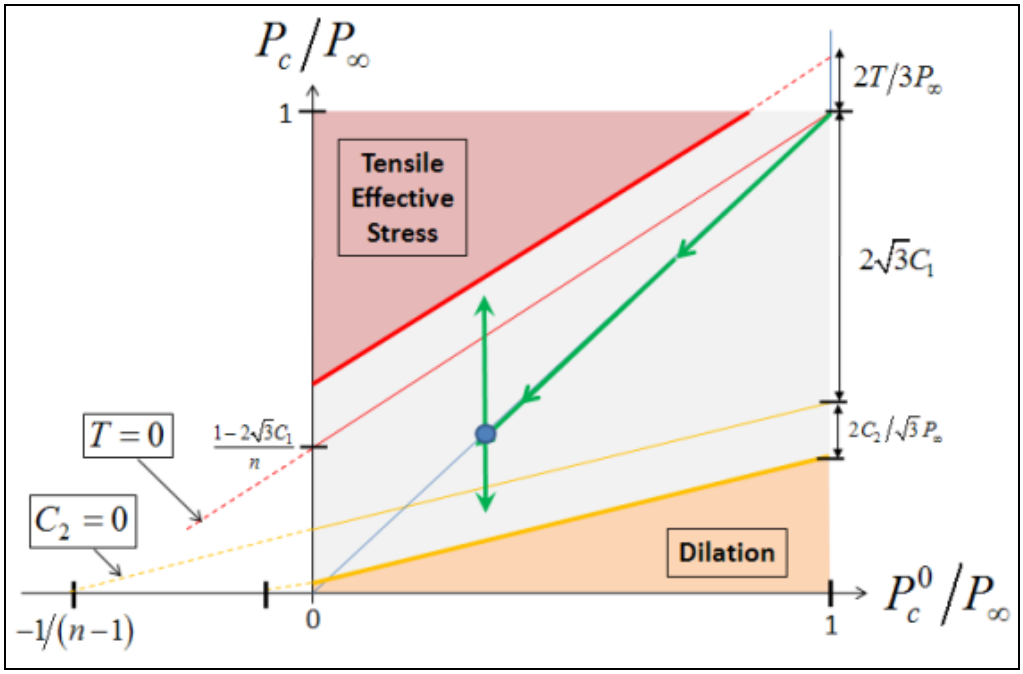

Figure 1. **Cavern pressure is decreased very slowly from geostatic pressure (P_∞) to some final value (P_c^0), after which the cavern pressure is increased rapidly (upward arrow) or decreased rapidly (downward arrow). The tensile effective stress or the dilation criteria, respectively, can be reached when pressure increase or decrease is large enough.**

This simple example is unrealistic for several reasons:

- It was assumed that steady state was reached before the cavern pressure change. A very long period of time is needed to reach steady-state.
- It is impossible to increase or decrease cavern pressure "instantaneously". In an actual gas cavern, several weeks are needed to reach maximum or minimum pressure. During this period, the high deviatoric stresses that characterize "elastic" behaviour are allowed enough time to partly release, and the criteria are reached later than predicted by the elastic computation, which is on the safe side. A more realistic assessment can be made only through numerical computation.

Numerical Computations

LOCAS software (Brouard et al., 2006), a finite element code developed by Brouard Consulting for simulating the thermo-hydro-mechanical behaviour of salt caverns and salt mines, was used for numerical computations. In this example, the cavern average depth is 1500 m, its height is 200 m and its volume is 500,000 m^3. The mesh used for numerical computation is shown on Figure 2; the cavern pressure history is represented on Figure 3. After a creation period lasting 2 years, during which cavern pressure decreases from geostatic (33 MPa) to halmostatic (18 MPa), the cavern is operated as a natural-gas storage. Each one-year cycle includes, sequentially:

- a 150-day period during which gas pressure is minimum ($P_{\min} = 8$ MPa — i.e., a pressure gradient of 0.0057 MPa/m or 0.25 psi/ft at the casing shoe), 1-2 on Figure 4;
- a $\Delta t_i -$ long period during which cavern pressure is built up to maximum pressure ($P_{\max} = 30$ MPa — i.e., a pressure gradient of 0.0204 MPa/m or 0.9 psi/ft at the casing shoe), 2-3-4 on Figure 4; and
- a $\Delta t_{\max} -$ long period during which gas pressure is kept constant, $P = P_{\max}$. (Various values of Δt_i and $\Delta t_{\max}$ are considered, but $\Delta t_i + \Delta t_{\max} = 150$ days.)

At the end of the cycle, cavern pressure is decreased to $P_{\min} = 8$ MPa over a 60-day period. The following several cases are considered.

1. The salt mass behaves according to the Norton-Hoff constitutive law (see the Appendix). The pressure build-up period is $\Delta t_i = 15$ days. The first cycle is considered.
2. The salt mass behaves according to the Norton-Hoff constitutive law. The pressure build-up period is $\Delta t_i = 30$ days. The first cycle is considered.
3. The salt mass behaves according to the Munson-Dawson constitutive law (see the Appendix). The pressure build-up period is $\Delta t_i = 30$ days. The first cycle is considered.
4. The salt mass behaves according to the Munson-Dawson constitutive law. The pressure build-up period is $\Delta t_i = 30$ days. The last (i.e., 16th) cycle is considered.
5. The salt mass behaves according to the Lemaitre-Menzel-Schreiner constitutive law (see the Appendix). The pressure build-up period is $\Delta t_i = 60$ days. The last (i.e., 16th) cycle is considered.

For the sake of simplicity, effects of cavern-temperature changes are not taken into account.

Considered Dilation Criterion

The considered dilation criterion is the RESPEC criterion (DeVries et al., 2005) which is defined as

$$\sqrt{J_2} < \sqrt{J_2}_{dil} = \frac{D_1 \left(\frac{I_1}{\operatorname{sgn}(I_1)\sigma_0} \right)^n + T_0}{\left(\sqrt{3}\cos\psi - D_2 \sin\psi \right)} \tag{9}$$

where $\sigma_0 = 1$ MPa is a dimensional constant, T_0 is the unconfined tensile strength of salt, ψ is Lode angle, and (D_1, D_2, n) are salt parameters. The selected parameters from Cayuta salt are given in Table 2.

The factor of safety (FOS) is defined as:

$$FOS = \frac{\sqrt{J_2}_{dil}}{\sqrt{J_2}} \tag{10}$$

And dilation appears when $FOS \le 1$.

Table 2 – Selected parameters for RESPEC dilation criterion.

Parameter	D_1 (MPa)	D_2	n	T_0 (MPa)
Value	0.773	0.524	0.693	1.95

General Comments

The value of the Factor of Safety (FOS) at the beginning of the low-pressure period is represented (Picture 1 on each of the following figures). The black stripe is the zone in which the dilation criterion is zero or close to zero. As expected, a dilatant zone, with thickness approximately equal to cavern radius, develops in the vicinity of the cavern (whatever constitutive law is selected).

The effective stress criterion is represented: (a) at the end of the minimum pressure period (Picture 2), when $P = P_{\min} = 8$ MPa; (b) during the pressure build-up period, when $P = 19$ MPa (Picture 3); and (c) at the end of the pressure build-up period, when $P = P_{\max} = 30$ MPa. The black stripe is the zone in which the effective stress criterion is zero or close to zero. Note that this criterion is written $\sigma_{\min} + P_c < 0 : \sigma_{\min}$ is the minimum compressive stress computed at any point of the rock mass, and P_c is the cavern pressure. (No attempt is made to compute the actual fluid (gas or brine) pressure inside the rock mass. The actual fluid pressure is likely to be smaller than P_c. In other words, the criterion is written correctly at the cavern wall; the criterion is too pessimistic when a point inside the rock mass is considered. The criterion over-estimates the extent of the effective tensile zone.)

Examples

1. The salt mass behaves according to the Norton-Hoff constitutive law (see the Appendix). The pressure build-up period is $\Delta t_i = 15$ days.

This example is represented on Figure 5. Salt dilation is observed at the beginning of the low-pressure period (Picture 1). At the end of this period, no tensile effective zone is observed (Picture 2). Effective tensile stresses develop in the upper part of the cavern wall 7.5 days after the pressure build-up began (Picture 3, gas pressure at this time is 19 MPa). At the end of this period, the zone experiencing tensile effective stresses is fully developed, but note that this zone does not include the cavern wall in the lower part of the cavern (Picture 4, gas pressure at this time is 30 MPa.)

2. The salt mass behaves according to the Norton-Hoff constitutive law. The pressure build-up period is $\Delta t_i = 30$ days. The first cycle is considered.

This example is represented on Figure 6. Pictures 1 and 2 are not represented, as they are identical to that in Example 1). There is no significant difference with Figure 5, which proves that the influence of the pressure build-up rate is small, at least in the two discussed examples.

3. The salt mass behaves according to the Munson-Dawson constitutive law (see the Appendix). The pressure build-up period is $\Delta t_i = 30$ days. The first cycle is considered.

The Munson-Dawson constitutive law includes a description of transient rheological behaviour. (The Norton-Hoff law did not.) In fact, a simplified version of the Munson-Dawson law was selected: only one creep mechanism is taken into account. No significant difference with the Norton-Hoff constitutive law is observed, except that the effective tensile zone at the end of the pressure build-up period is slightly larger (Figure 7, Picture 4).

4. The salt mass behaves according to the Munson-Dawson constitutive law. The pressure build-up period is $\Delta t_i = 30$ days. The last (or 16^{th}) cycle is considered.

The cumulative effect of the cycles is clear: while the dilatant zone is slightly smaller than before, the effective tensile zone is larger (Figure 8, Pictures 1, 3 and 4).

5. The salt mass behaves according to the Lemaitre-Menzel-Schreiner constitutive law (see the Appendix). The pressure build-up period is $\Delta t_i = 60$ days. The last cycle is considered.

The Lemaitre-Menzel-Schreiner includes strain-hardening. (When a sample is submitted to a constant mechanical loading (creep test), the axial strain rate slowly decreases with time.) Direct comparison with the former examples is difficult. It can be observed (Figure 9, Pictures 3 and 4) that the extension of the effective tensile zone is smaller.

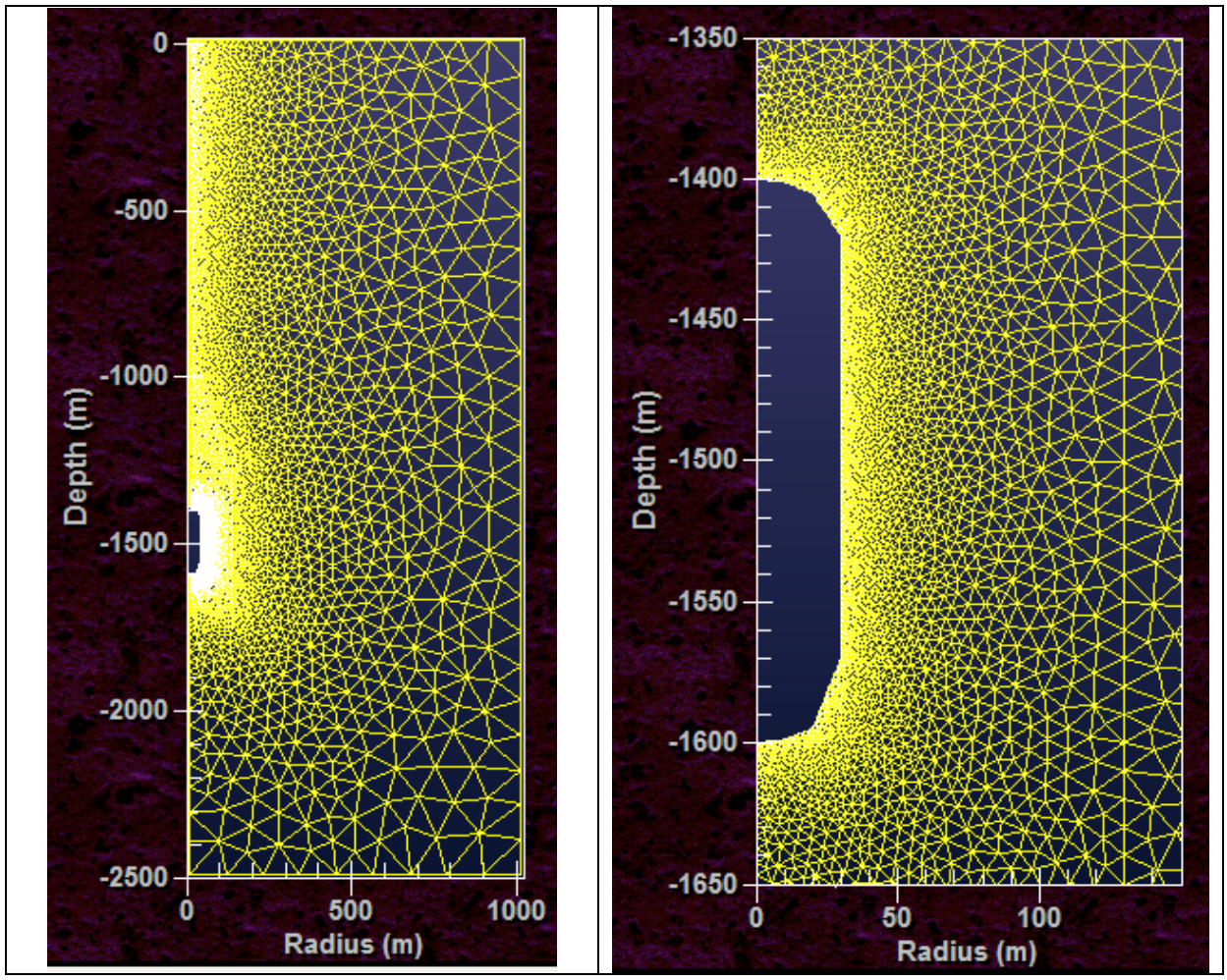

Figure 2. Mesh used for numerical computations.

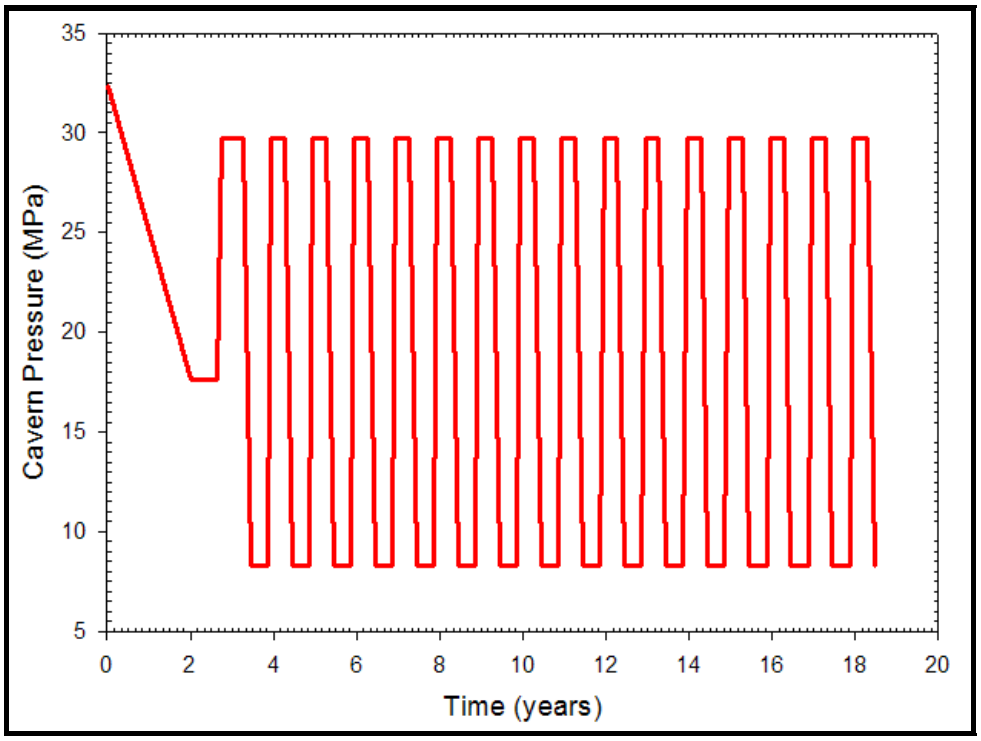

Figure 3. Cavern pressure evolution, 15 pressure cycles.

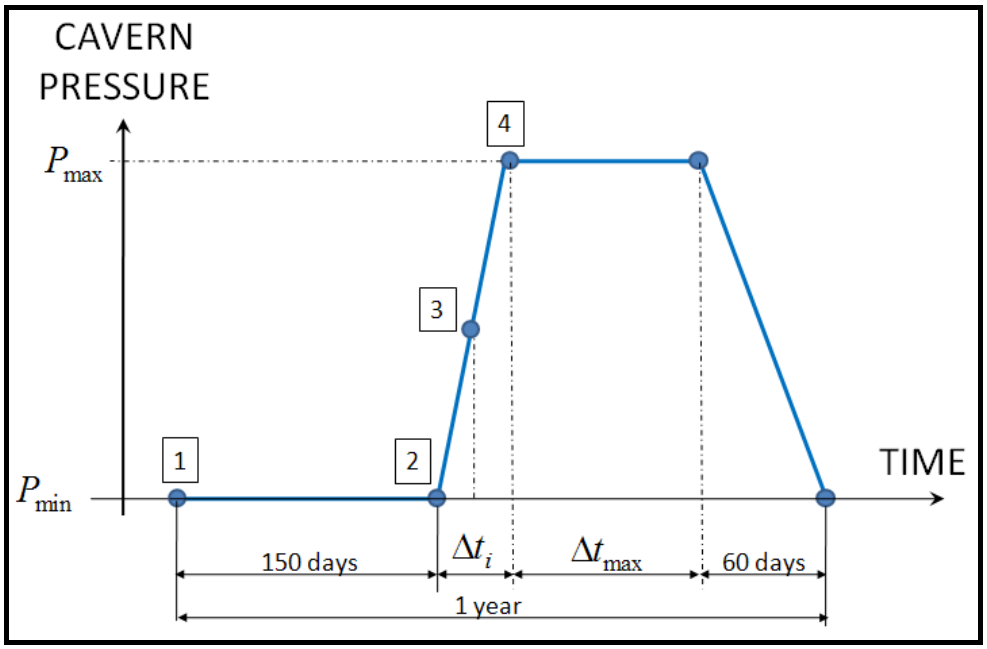

Figure 4. Pressure cycle.

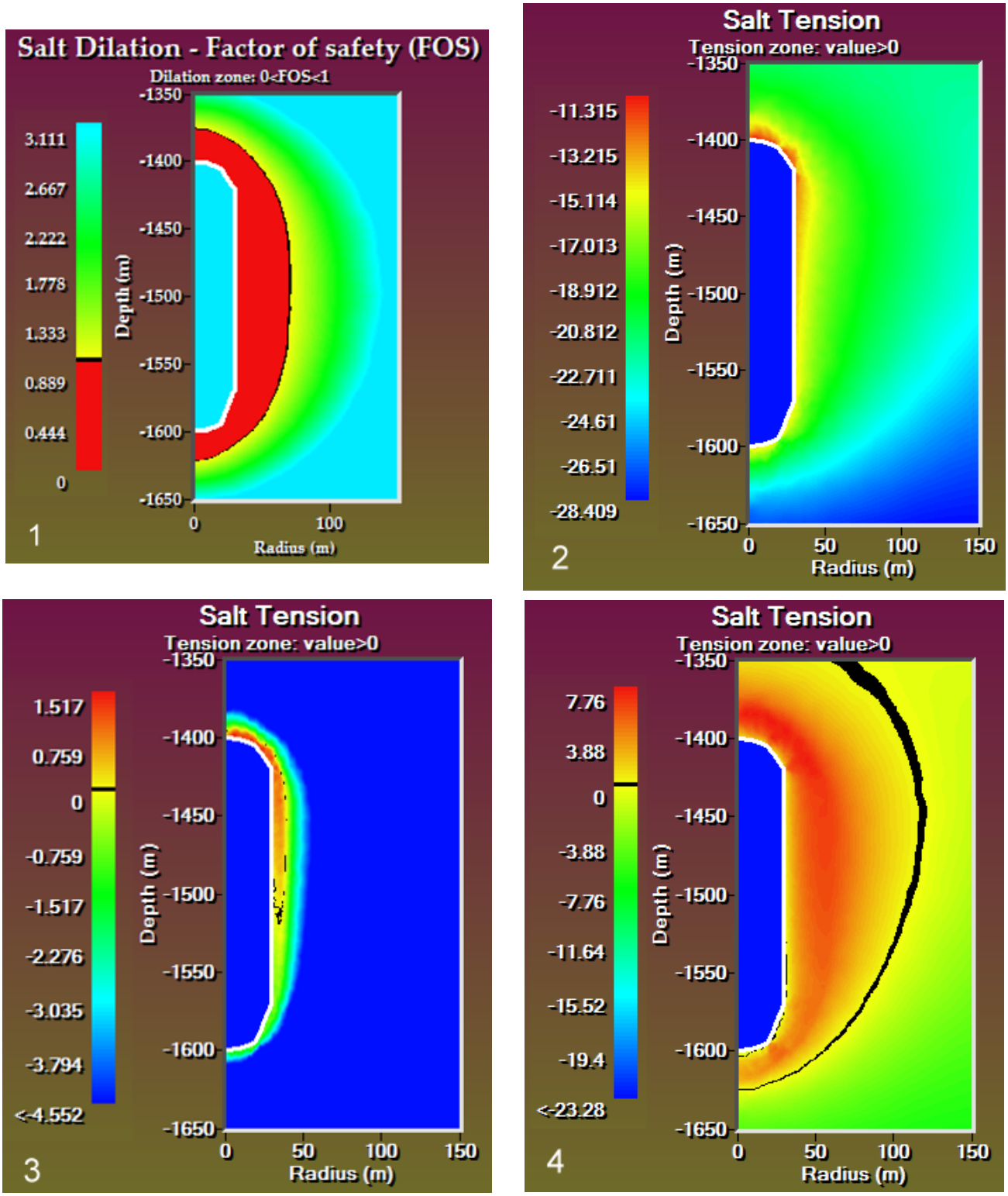

Figure 5. **Norton-Hoff creep law, Dilation and effective stress criteria, Pressure increase completed in 15 days, First pressure cycle.**

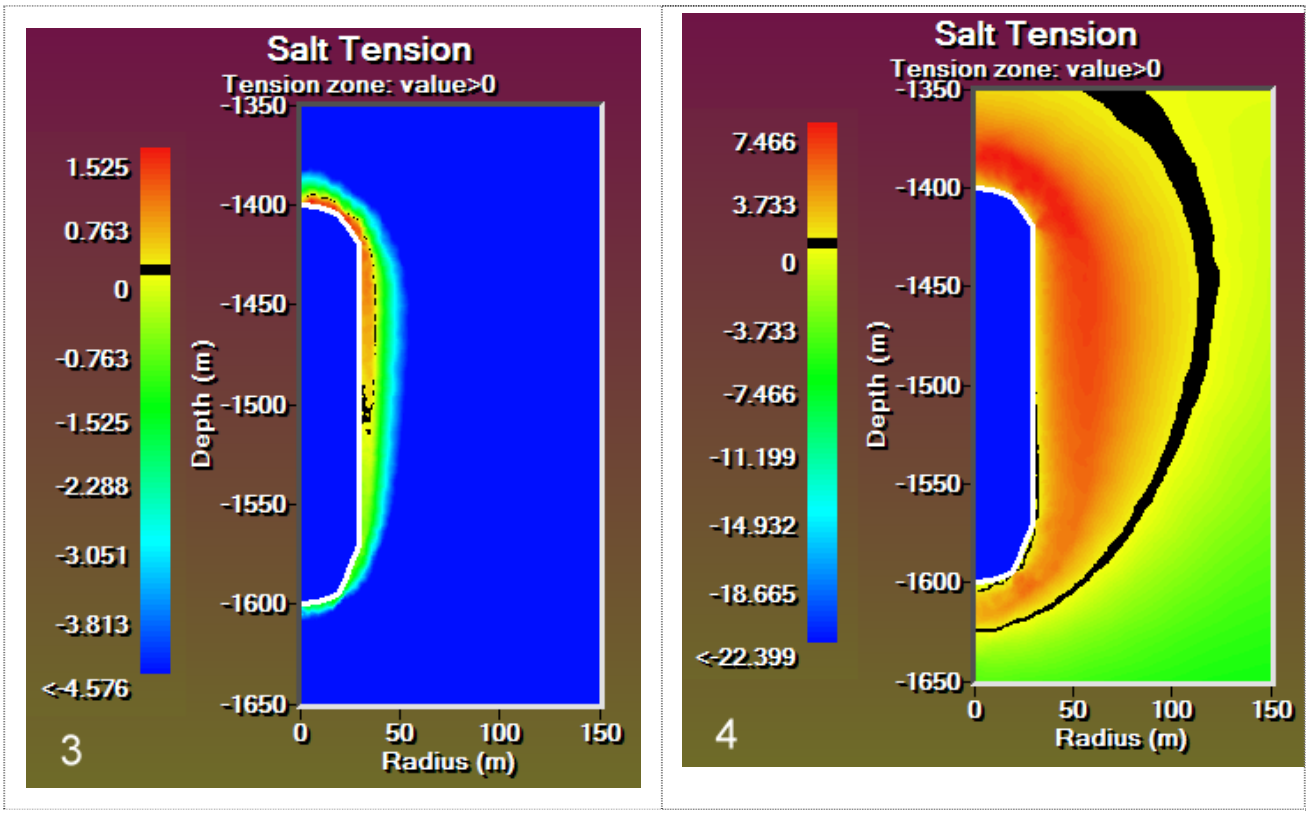

Figure 6. **Norton-Hoff creep law, Effective stress criterion, Pressure increase completed in 1 month, First pressure cycle.**

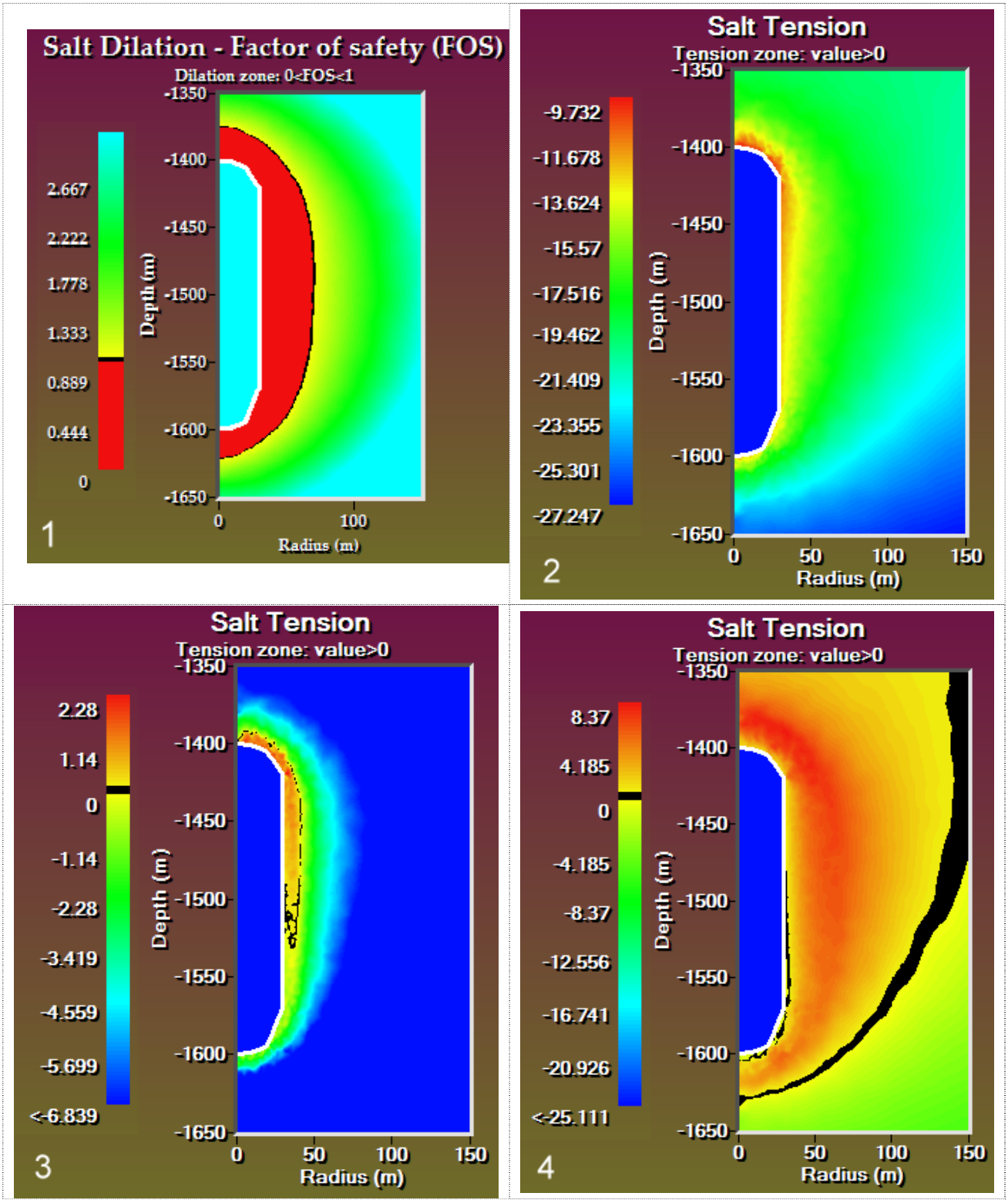

Figure 7. **Munson-Dawson law, Dilation and effective stress criteria, Pressure increase completed in 1 month, First pressure cycle.**

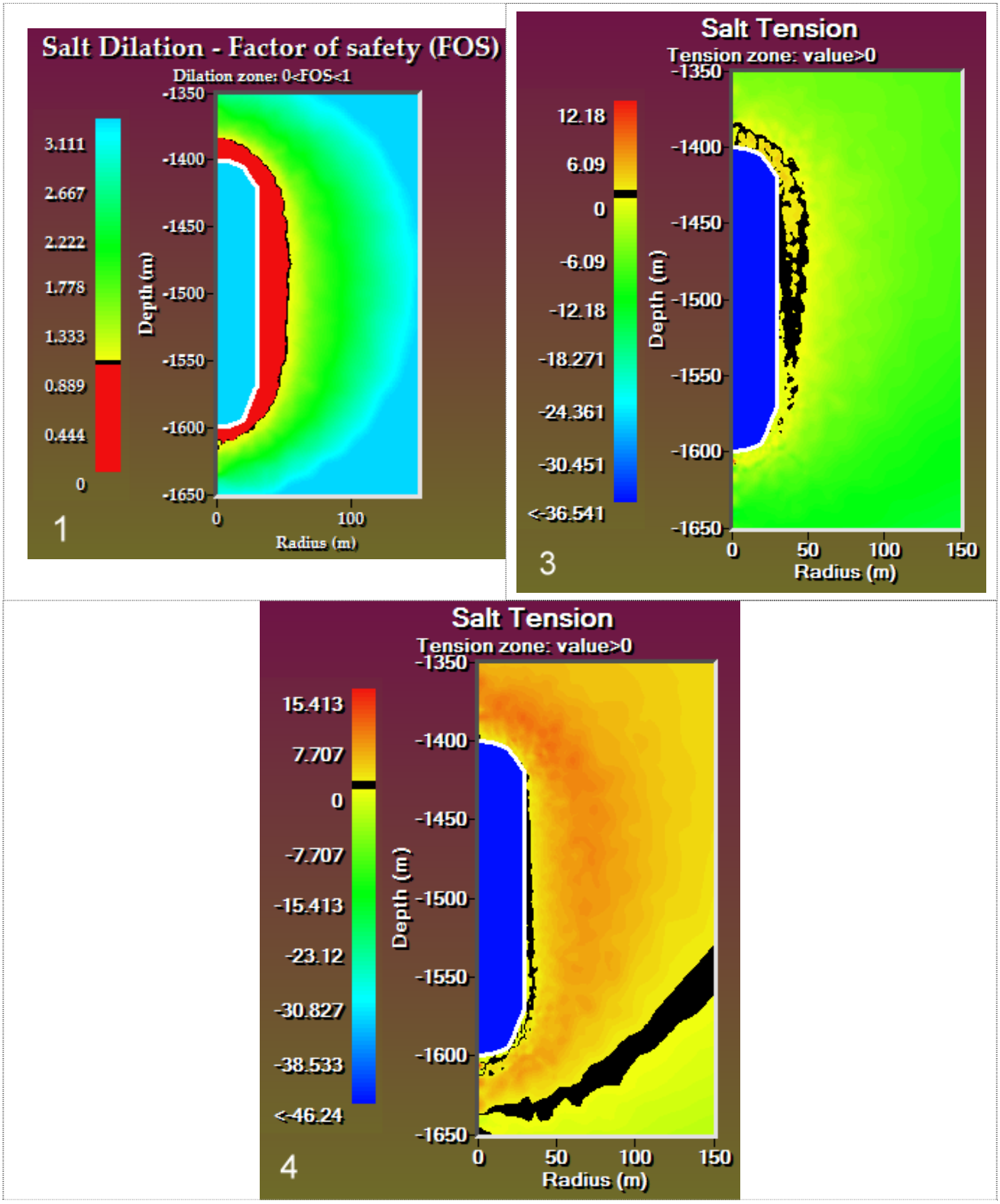

Figure 8. **Munson-Dawson law, Dilation and effective stress criteria, Pressure increase completed in 1 month, Last pressure cycle.**

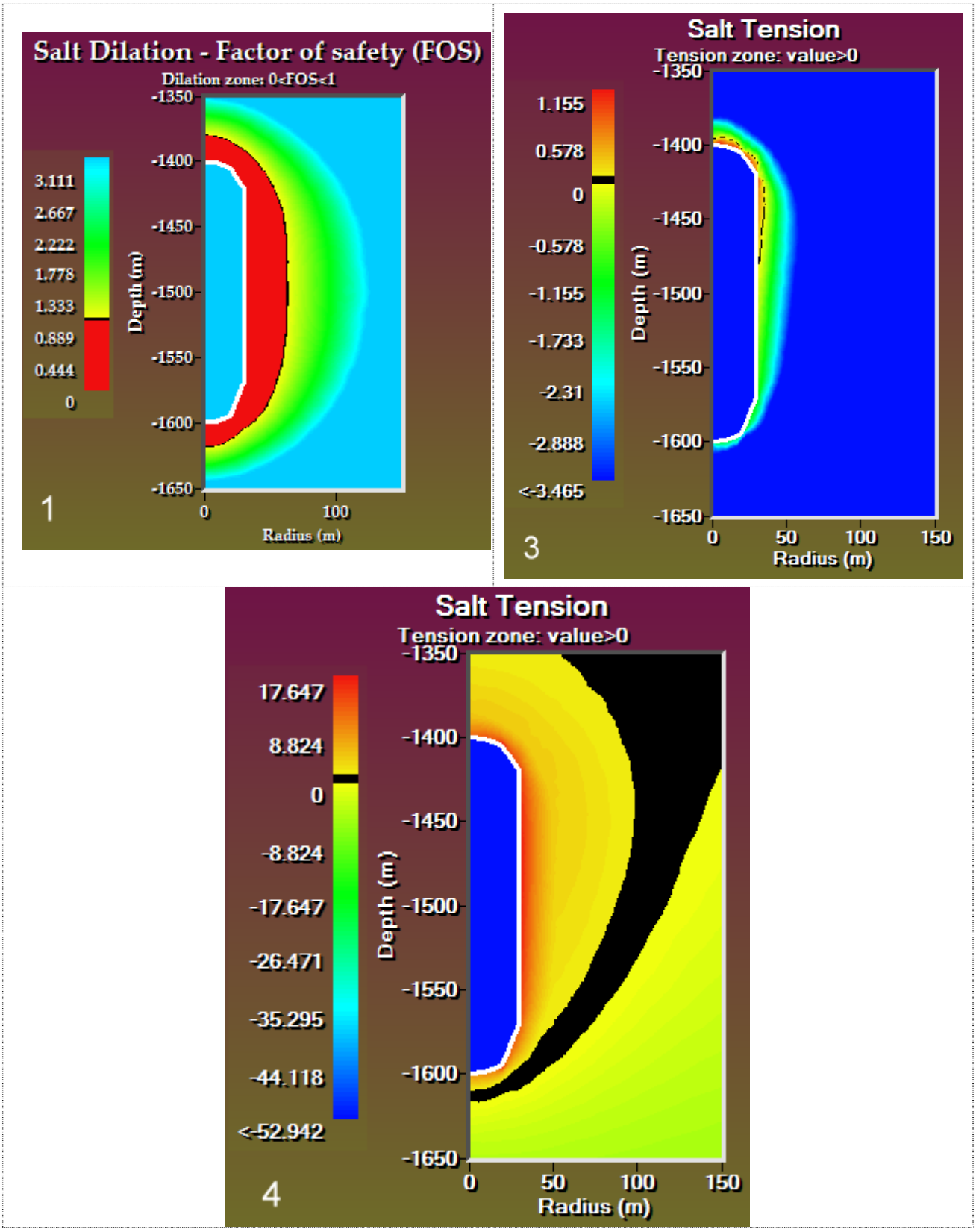

Figure 9. **Lemaitre-Menzel-Schreiner law, Dilation and effective stress criteria, Pressure increase completed in 2 months, Last pressure cycle.**

Conclusion

It was proved that, in a gas-storage cavern submitted to large pressure cycles, a tensile effective zone develops at the cavern wall during gas pressure build-up. This phenomenon originates in the stress redistribution that occurs when gas pressure is minimal. During such a phase, the deviatoric stress slowly decreases in the rock mass, and the difference between the tangential stresses and the radial stress decreases accordingly. At the end of such a period, when gas is injected again in the cavern, large elastic stresses develop at the cavern wall, and the overall tangential stresses become larger than the normal stress, resulting in tensile effective stresses at cavern wall. The computations presented in this paper are pessimistic, in that (1) no tensile strength is considered, and (2) fluid pressure is assumed to equal the cavern gas pressure in the rock mass.

The practical consequences of this result are still to be assessed. It is reasonable to assume that some micro-permeation takes place at the cavern wall and that some gas seeps through the rock mass. The gas penetration depth must be assessed and further investigations conducted.

REFERENCES

Bauer S.J., Ehgartner B.L. and Neal J.T. *Geotechnical Studies Associated with Decommissioning the Strategic Petroleum Reserve Facility at Weeks Island, Louisiana: A Case History*. *Proc. Technical Class and Technical Session SMRI Fall Meeting*, San Antonio, pp. 146-156 (2000).

Bérest P., Brouard B. and de Greef V. *Salt Permeability Testing*. SMRI Research Project No. 2001-1 (2001a).

Bérest P., Brouard B. and de Greef V. *Executive Summary Salt Permeability Testing – The Influence of Permeability and Stress on Hollow Salt Samples*. SMRI Research Project No. 2001-8 (2001b).

Bérest P., Brouard B., Feuga B. and Karimi-Jafari M. *The 1873 Collapse of the Saint-Maximilien panel at the Varangéville salt mine*. Submitted to Int. J. Rock Mech. Min. Sc. (2007).

Brouard B., Karimi-Jafari M., Bérest P. and Frangi A. *Using LOCAS Software to Better Understand the Behavior of Salt Caverns*. In Proc. S.M.R.I. Spring Meeting, Brussels, Belgium, pages 273-288, 2006.

DeVries K.L., Mellegard K.D. and Callahan G.D. *Cavern Design Using a Salt Damage Criterion: Proof-of-Concept Research Final Report*. Proc. SMRI Spring Meeting, Houston, pp. 1-18. (2003)

DeVries K.L., Mellegard K.D., Callahan G.D. and Goodman W.M. *Cavern Roof Stability for Natural Gas Storage in Bedded Salt*. Report RSI-1829, prepared by RE/SPEC Inc., Rapid City, SD, for United States Department of Energy, National Energy Technology Laboratory, Pittsburgh, PA (2005).

DeVries K.L. *Geomechanical Analyses to Determine the Onset of Dilation Around Natural Gas Storage Caverns in Bedded Salt*. Proc. SMRI Spring Meeting, Brussels, pp.131-150 (2006).

Fokker PA. *The behavior of salt and salt caverns*. PhD Thesis, Delft University of Technology, The Netherlands (1995).

Kamlot P., Günther R.M., Stockmann N. and Gärtner G. *Modeling of strain softening and dilatancy in the mining system of the southern flank of the Asse II mine*. Proc.6th Conf. Mech. Beh. Salt, Taylor & Francis Group, London, pp. 327-336 (2007).

Lux K.H., Düsterloh U. and Wolters R. *Long-term Behavior of Sealed Brine-filled Cavities in Rock Salt Mass- A new Approach for Physical Modeling and Numerical Simulation*. Proc. SMRI Fall Meeting, Rapid City, pp. 105-133 (2006).

Malinsky L. *Evaluation of Salt Permeability Tests*. SMRI Research Project Report No. 2001-4-SMRI (2001).

Minkley W., Mülhbauer J. and Storch G. *Dynamic processes in salt rocks – a general approach for softening processes within the rock matrix and along bedding planes*. Proc. 6th Conf. Mech. Beh. Salt, Taylor & Francis Group, London, pp. 295-303 (2007).

Munson D.E. *Correlation of Creep Behavior of Domal Salts*. Proc. SMRI Spring Meeting, Las Vegas, pp. 3-27 (1999).

Nieland J.D. and Ratigan J.L. *Geomechanical Evaluation of Two Gulf Coast Natural Gas Storage Caverns*. Proc. SMRI Spring Meeting, Brussels, pp. 61-89 (2006).

Popp T., Brückner D. and Wiedemann M. *The gas frac scenario in rock salt – implications from laboratory investigations and filed studies*. Proc. SMRI Spring Meeting, Basel, pp. 288-305 (2007).

Ratigan J.L., Van Sambeek L.L., DeVries K.L. and Nieland J.D. *The influence of Seal Design on the Development of the Disturbed Rock Zone in the WIPP Alcove Seal Tests*. Report RSI-0400, prepared by RE/SPEC Inc., Rapid City, SD, for Sandia National Laboratories, Albuquerque, NM (1991).

Rokhar R.B., Staudtmeister K. and Zander-Schiebenhöfer D. *Development of a New Criterion for the Determination of the Maximum Permissible Internal Pressure for Gas Storage Caverns in Rock Salt*. Final Report of SMRI Research Project No. 97-0001-SMRI (1997).

Rokhar R.B., Staudtmeister K. and Zander-Schiebenhöfer, D. *High Pressure Cavern Analysis*. Proc. SMRI Spring Meeting, Houston, pp. 88-113 (2003).

Rokahr R.B., Staudtmeister K and Zander-Schiebenhöfer D. *Application of a Continuum Damage Model for Cavern Design Case Study: Atmospheric Pressure*. Proc. SMRI Spring Meeting, Wichita, Kansas, pp. 38-55 (2004).

Spiers J.C., Peach C.J., Brzesowsky R.H., Schutjens T.M., Liezenberg J.L. and Zwart H.J. *Long Term Rheological and Transport Properties of Dry and Wet Salt Rocks*. Report EUR 11848, prepared for Commission of the European Communities, by University of Utrecht, Utrecht, The Netherlands (1988).

Stormont J.C. *Evaluation of Salt Permeability Tests*. SMRI Research Project Report No.2001-2-SMRI (2001).

APPENDIX

- **Norton-Hoff Law**

$$\dot{\varepsilon}_{ij} = A\exp\left(-\frac{Q}{RT}\right)\frac{1}{n+1}\frac{\partial}{\partial\sigma_{ij}}\left(\sqrt{3J_2}\right)^{n+1}$$

where T is absolute temperature (K) of salt.

The parameters set for Bayou Choctaw salt are:

$$A = 64.03 \text{ /MPa}^{4.06}\text{-year} \quad n = 4.06 \quad Q/R = 5956 \text{ K}$$

- **Munson-Dawson Law**

$$\dot{\varepsilon}_{ij}^{vp} = F\dot{\varepsilon}_{ij}^{ss} \qquad \begin{aligned} F &= e^{\Delta(1-\varsigma/\varepsilon_t^*)^2} \quad \text{when} \quad \varsigma \le \varepsilon_t^* \\ F &= e^{-\delta(1-\varsigma/\varepsilon_t^*)^2} \quad \text{when} \quad \varsigma \ge \varepsilon_t^* \end{aligned}$$

$$\dot{\varsigma} = (F-1)\dot{\varepsilon}^{ss}, \quad \dot{\varepsilon}^{ss} = A_2\exp\left(-\frac{Q_2}{RT}\right)\left(\sqrt{3J_2}\right)^{n_2}$$

$$\dot{\varepsilon}_{ij}^{ss} = \frac{3\dot{\varepsilon}^{ss}}{2\sqrt{3J_2}}s_{ij} \qquad \varepsilon_t^* = K_0 e^{cT}\sigma^m \text{ and } \Delta = \alpha + \beta Log_{10}\sigma/\mu$$

The parameters set for soft salt (After Munson, 1999) are:

$$A_2 = 11.32\cdot 10^{12} \text{ /s} \quad Q_2/R = 5032 \text{ K} \quad n_2 = 5 \quad \delta = 0.58 \quad \mu = 12.4 \text{ GPa}$$

$$m = 3 \quad c = 9.198\cdot 10^{-3} \quad \alpha = -17.37 \quad \beta = -7.738 \quad K_0 = 6.275\cdot 10^5$$

- **Lemaitre-Menzel-Schreiner Law**

$$\dot{\varepsilon}_{ij}^{vp} = \frac{\partial}{\partial t}(\zeta)^{\alpha}\frac{\partial}{\partial\sigma_{ij}}\left(\sqrt{3J_2}\right) \qquad \dot{\zeta} = \left(\frac{\sqrt{3J_2}}{K}\right)^{\beta/\alpha}$$

The selected parameter set is:

$$\alpha = 0.21 \quad \beta = 2.55 \quad K = 1.075 \text{ MPa}.$$